

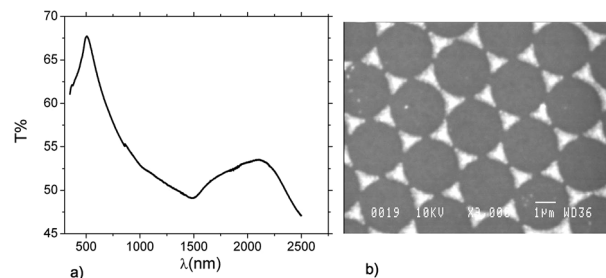
PAPER

1

Nonlinear optical enhancement caused by a higher order multipole mode of metallic triangles

Monique van der Veen,* Gilles Rosolen, Thierry Verbiest, Maarten K. Vanbel, Bjorn Maes and Branko Kolaric*

We describe a nonlinear optical study of gold triangles that exploits a higher order plasmonic resonance.



Please check this proof carefully. **Our staff will not read it in detail after you have returned it.**

Translation errors between word-processor files and typesetting systems can occur so the whole proof needs to be read. Please pay particular attention to: tabulated material; equations; numerical data; figures and graphics; and references. If you have not already indicated the corresponding author(s) please mark their name(s) with an asterisk. Please e-mail a list of corrections or the PDF with electronic notes attached - do not change the text within the PDF file or send a revised manuscript. Corrections at this stage should be minor and not involve extensive changes. All corrections must be sent at the same time.

Please bear in mind that minor layout improvements, e.g. in line breaking, table widths and graphic placement, are routinely applied to the final version.

We will publish articles on the web as soon as possible after receiving your corrections; **no late corrections will be made.**

Please return your **final** corrections, where possible within **48 hours** of receipt by e-mail to: materialsC@rsc.org

Queries for the attention of the authors

Journal: Journal of Materials Chemistry C

Paper: c4tc02427c

Title: Nonlinear optical enhancement caused by a higher order multipole mode of metallic triangles

Editor's queries are marked like this... **1**, and for your convenience line numbers are inserted like this... 5

Please ensure that all queries are answered when returning your proof corrections so that publication of your article is not delayed.

Query Reference	Query	Remarks
1	For your information: You can cite this article before you receive notification of the page numbers by using the following format: (authors), J. Mater. Chem. C, (year), DOI: 10.1039/c4tc02427c.	
2	Please carefully check the spelling of all author names. This is important for the correct indexing and future citation of your article. No late corrections can be made.	
3	Please check that the inserted GA image and text are suitable.	
4	"Kolloch" is not cited as an author of ref. 13. Please indicate any changes that are required here.	
5	Ref. 4: Can this reference be updated?	

Nonlinear optical enhancement caused by a higher order multipole mode of metallic triangles†

Cite this: DOI: 10.1039/c4tc02427c

Monique van der Veen,^{*ab} Gilles Rosolen,^c Thierry Verbiest,^a Maarten K. Vanbel,^a Bjorn Maes^c and Branko Kolaric^{*d}

We describe a nonlinear optical study of gold triangles that exploits a higher order plasmonic resonance. A comprehensive nonlinear optical characterisation was performed both by second harmonic generation (SHG) and two photon fluorescence spectroscopy (2PF). We demonstrate and explain the enhancement of the coherent and incoherent nonlinear optical emission by a higher order multipolar mode of the plasmonic structure. The peculiarities of the mode shape and its influence on intensity and polarisation of the nonlinear signal are experimentally and numerically confirmed.

Received 24th October 2014
Accepted 10th December 2014

DOI: 10.1039/c4tc02427c

www.rsc.org/MaterialsC

I. Introduction

Localized surface plasmon polaritons (LSPPs) and surface plasmon polaritons (SPPs) are electromagnetic excitations coupled to the electron charge density waves localized on metallic nanostructures and metal–dielectric interfaces, respectively. These modes allow for confinement of light at the nanoscale level (10–100 nm), far below conventional optics.^{1,2} Additionally, in modern nano-optics plasmonic resonances become important as they offer a unique and distinctive way for controlling light emission by coupling radiation of a nanoprobe (molecule, quantum dot *etc.*) with the environment.^{3,4,5}

Recently, nonlinear optical effects attract special attention as strong electromagnetic fields in the vicinity of metallic structures generate a significant enhancement of the nonlinear processes, which depend super-linearly on the local fields.² Moreover, the ability to convert low-energy quanta into a quantum of higher energy is crucial for a variety of applications, including bioimaging, drug delivery, photovoltaics and solar cell technology.² However, the majority of reported optical studies considering metallic particles and their arrays have been performed only in the linear optical regime using transmission, reflection and fluorescence spectroscopy.^{6,7,8} Up to

now, a number of metallic nanostructures of diverse architectures have been studied by nonlinear optical techniques.^{2,9,10}

Structures such as gold metallic triangles (*i.e.* curved nano-triangles and nanoprisms) attract interest because of their antenna effect. The latter effect creates a huge enhancement of electromagnetic fields in the vicinity of tips.^{10,14,15,16} Furthermore, recent investigations of gold triangles point out the mutual importance of the resonance position and tip-to-tip orientation for their optical response.^{13,14,19} Recently, plasmonic circuitry at the micrometer scale made from metallic nanotriangles and nanoprisms was demonstrated with potential applications in telecommunication technology.^{17,18} Likewise, it has been indicated^{2,10} that nanotriangles are promising candidates for various applications such as photonic circuits, super-resolution imaging, enhanced fluorescence and Raman detection.

Despite a tremendous number of publications, the higher order modes are seldom examined and the dipolar mode is preferentially used for enhancement of an optical signal.^{2,20,21} However, for various potential applications (especially for sensing using linear or nonlinear emission) the dipole mode is probably a less attractive resonance, because the strong electric field generated by incoming light (matching between dipole mode and fundamental wavelength) can trigger nanopatterning processes.^{20,22,23}

In this article a comprehensive nonlinear optical study of gold metallic triangles is described using two different nonlinear optical techniques, coherent second harmonic generation (SHG) and incoherent two-photon fluorescence (2PF) spectroscopy. With these two techniques we are able to reveal the effect of the higher order and less studied mode on the enhancement of the coherent and incoherent nonlinear emission.

II. Results and discussion

The triangular gold nanoparticles in this study are made by nanosphere lithography utilising the drop coating method of

^aDepartment of Chemistry, University of Leuven, Celestijnenlaan 200D, B-3001 Heverlee, Belgium. E-mail: M.A.vanderVeen@tudelft.nl

^bCatalysis Engineering, Applied Sciences, Delft University of Technology, Julianalaan 136, 2628 BL, Delft, The Netherlands

^cMicro- and Nanophotonic Materials Group, Faculty of Science, University of Mons, 20 Place du Parc, B-7000 Mons, Belgium

^dLaboratoire Interfaces and Fluides Complexes, Centre d'Innovation et de Recherche en Matériaux Polymères, University of Mons, 20 Place du Parc, B-7000 Mons, Belgium. E-mail: branko.kolaric@umons.ac.be

† Electronic supplementary information (ESI) available. See DOI: 10.1039/c4tc02427c

Micheletto^{11,12} as used by Kolaric and Morarescu.¹³ The technique employs nanospheres dispersed in solution to create a close-packed monolayer with hexagonal symmetry, which is employed as a mask in a subsequent step, where gold is deposited (40 nm) through the nanospheres to fill the void spaces in the layer lattice. Regular arrays of triangular gold nanoparticles are fabricated in a last step, when the nanosphere mask is removed. The corresponding metallic triangles (Fig. 1b) were chosen due to the relatively good matching between the higher order plasmonic resonance and the wavelength of the fundamental.

A top-view scanning electron microscope (SEM) image (Fig. 1b) shows the size and the shape of the metallic triangles (side ~ 900 nm) as well as the exceptionally good ordering of triangles within the array. The optical properties of metallic particles are influenced by the particle size and orientation. Therefore, by increasing the size a higher order plasmon mode appears in the extinction spectrum (Fig. 1a).^{13,23,25,26} Additionally, the higher order plasmon bandwidth can become broader as a result of more radiative damping. In our case, the transmission spectrum of the gold metallic triangles (Fig. 1a) consists of two main dips (and thus extinction maxima): a small dip (between 500 nm and 1800 nm, with a minimum around

1500 nm), originating from a higher order mode of the triangles, and a main dip (above 2500 nm) in the near infrared domain, related to the dipole mode.¹³ The dipolar minimum is beyond our experimental data, however these dipole and higher order modes have also been identified in previous work.¹³ In the article published by Morarescu *et al.*, dipolar and higher order modes of nanotriangles of different size are fully described and discussed.

The nonlinear optical study of the gold triangles was performed using a wide field nonlinear optical microscope.^{27,28} Fig. 2a shows an optical image of the array studied in our experiments, while the nonlinear responses are recorded by imaging 2PF and SHG as a function of polarisation (Fig. 2b and c, respectively). The wavelength of the fundamental (800 nm) overlaps with the broadband higher order mode resonance of the gold triangle. Furthermore, Fig. 2 confirms that the observed enhancement is not related to the presence of a local defect within the array (the yellow line indicates a defect).

Fig. 2b and c show merged 2PF- and SHG-images, which consist of three combined images with different colour, where each colour corresponds to a different plane of polarisation of the incident light. The depicted incident polarisations are chosen such that they coincide with an orientation of the triangle edges. These images indicate that each triangle tip generates the nonlinear optical light independently: the response of each tip is spatially resolved from the responses of the other two tips of the same triangle, as well as from the tip of the neighbouring triangles. The pattern of the array is clearly visible in the nonlinear response, pointing out that the observed response is directly related to the plasmonic structure itself. The figure shows a defect in the Au-triangle array (see yellow line as guide to the eye) where no SHG and 2PF is generated. In fact the intensity along this defect corresponds to the noise level in the SHG and 2PF images. With regard to the standard deviation of this noise level the detected SHG and 2PF intensity of the triangle tips is on average 10 and 65 times higher. As we can not detect the SHG and 2PF generated by the bulk of the faulty

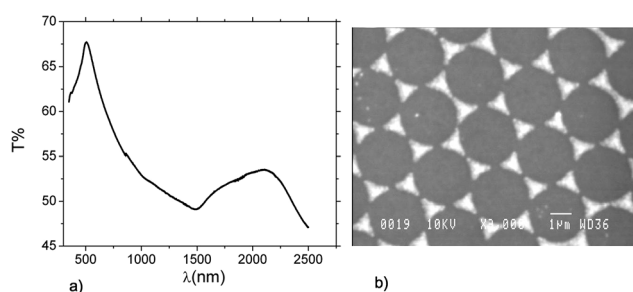


Fig. 1 (a) Measured transmission spectrum of the gold triangle array. (b) SEM image of the array, with the 1 μ m scale bar.

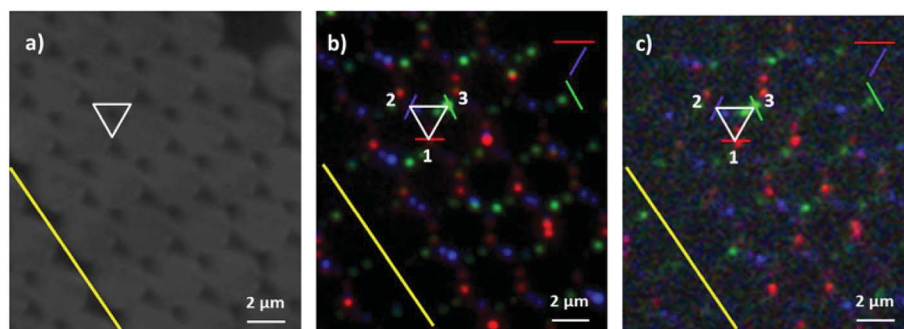


Fig. 2 (a) Optical image. (b) Merged image of three different measured 2PF-images or (c) SHG images, respectively, each taken with a different plane of polarisation of the incident light. The incident polarisation plane of the blue, red and green images are depicted by a line on the image in these respective colours. As a guide to the eye, the white triangle corresponds in each of the three images. In (b) and (c) the tips of the drawn triangle are decorated with the direction of the plane of polarisation that corresponds to the highest 2PF or SHG-intensity for that tip. Note that schematic presentation of the structure, the drawn white triangles are displayed larger than actual, in order that all light generated by triangles be presented with the drawings. The yellow line is a guide to the eye to show a defect in the Au-triangle array. Along this defect, no 2PF and SHG is detected.

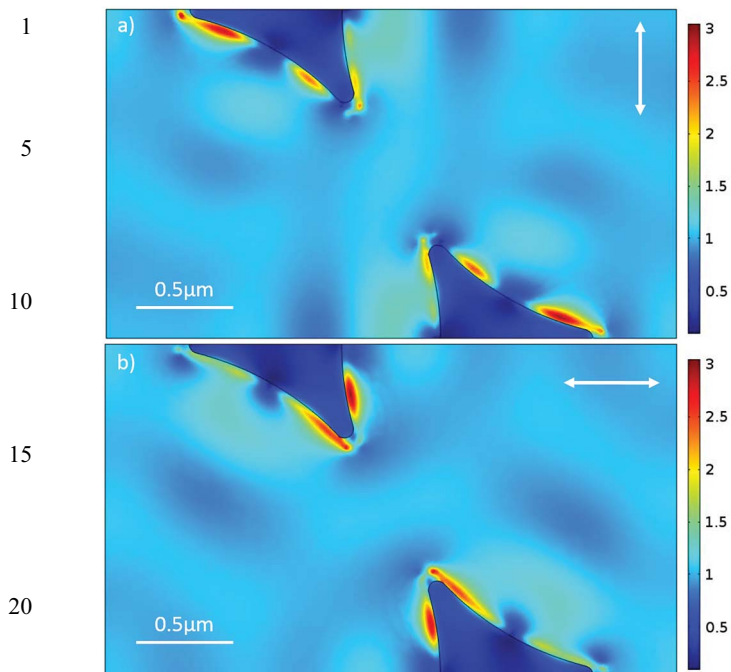


Fig. 3 Simulated electric field enhancement profile in a plane 20 nm above the substrate. (a) For vertically incident polarisation and (b) for horizontally incident polarisation. The white arrows indicate the respective polarisation of the incident wave. The light has a wavelength of 800 nm and is perpendicularly incident on the substrate.

structures, and as the SHG and 2PF generated by the tips is spread out over a spot the size of the diffraction limit, the numbers are an underestimation of the effective enhancement factor. Since the higher order and dipole mode are very well separated in our structure (over 1000 nm in wavelength), the

recorded images are direct observations of the nonlinear enhancement caused by the higher order mode.

Fig. 2 also shows that both SHG and 2PF are most effectively generated when the plane of polarisation of the incident light is oriented perpendicularly to the direction of the tip. This ‘puzzling’ polarisation dependence of the nonlinear response was noted before, in the context of femtosecond laser patterning using nanostructures and larger sized metallic triangles.^{22,24} However, in the case of the nanostructures studied by Valev *et al.*²⁴ the detected polarisation dependence is explained by the fact that the laser induces melting of the structure on the local scale, causing elongation of the nanostructures (formation of a resonant cavity). Thus, depending on the wavelength of light and the length of the cavity, different plasmon resonance modes could be excited. However, this finding was not specially emphasised in the article²⁴ since the authors’ primary objective was to explain the origin of the light induced nanopatterns (nanobumps). Additionally, Kolloch *et al.*²² describes nanopatterning of gold triangles and the effect of a particular resonance (dipolar and higher order mode) on nanopattern formation. In the case when the wavelength of the laser matches with a higher order mode plasmonic resonance, Kolloch *et al.*²² observed the same unusual polarisation dependence, quite different from polarisation dependence caused by dipole mode enhancement.¹³ Since nanopatterning did not occur in our study, it is likely that the observed polarisation dependence of the nonlinear response is caused by the effect of the higher order mode.

Here we also note that we tried to study smaller metallic triangles, with 135 nm edge length (made from spheres with radius 630 nm (ref. 13)), that exhibit a nice matching between the fundamental wavelength and the dipolar response. However, the nonlinear optical intensity decreased during the

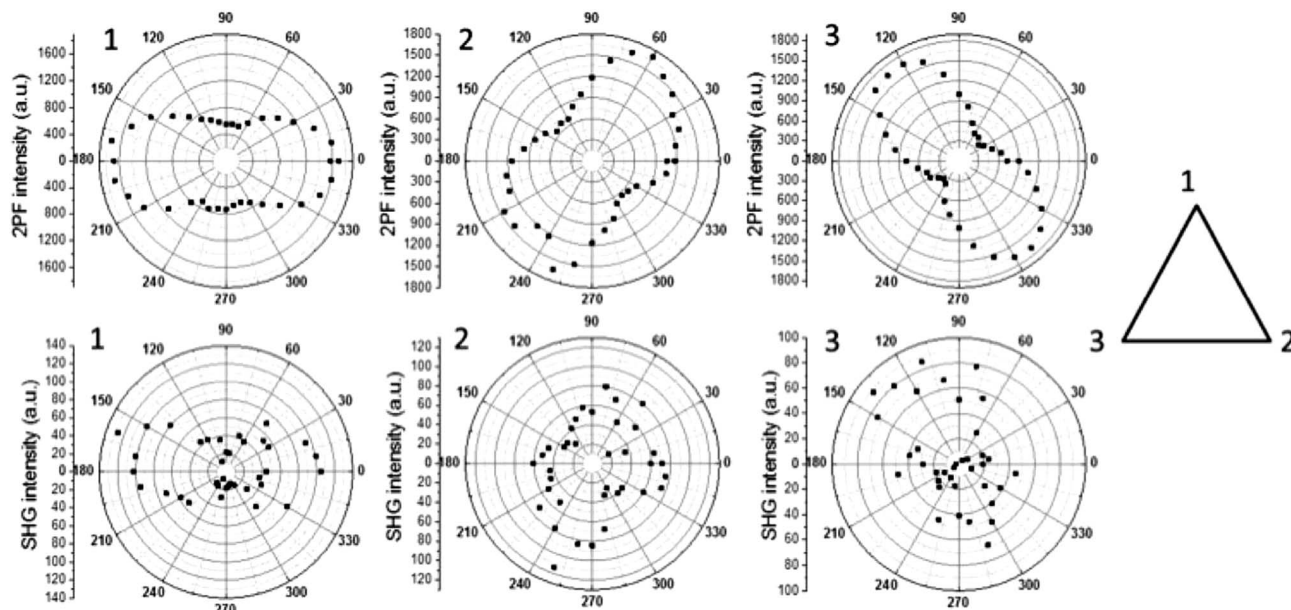


Fig. 4 (Top row) Measured 2PF intensity and (bottom row) SHG intensity in function of the polarisation angle of the incident light. The numbers assign for which tip of the metallic triangle the 2PF or SHG intensity is shown, see the sketch on the right.

measurement, indicating that the sample changed under irradiation (melted or patterned). This observed nanopatterning made it impossible for us to perform a full nonlinear optical study using dipolar modes of metallic triangles.

To clarify these results the near-field optical properties of the same triangular array have also been numerically studied. Fig. 3 shows the calculated electric field profile (more specifically the module of the enhanced field, which is the total field divided by the incident field) for a vertically incident plane wave at a wavelength of 800 nm, with two perpendicular incidence polarisations (white arrows in Fig. 3a and b, respectively). These profiles can be attributed to the excitation of a higher order mode. Indeed, it is clearly visible that the largest fields are generated on the triangular tips that are aligned perpendicular to the polarisation direction. The fundamental dipole-like resonance has maxima at opposite ends of the triangles (which 'samples' or feels the complete triangle), but for these (relatively large) particles this resonance happens at much larger wavelengths simulations show the fundamental resonance at 2.55 μm , see ESI† for the dipolar field profile at this wavelength in function of the incident polarisation. At smaller wavelengths, such as 800 nm as in Fig. 3, the particle will resonate over a smaller typical length scale (only a part of the triangle), which is possible by sampling sections in-between the extremities of the triangle, so that the hot-spots are not at the 'typical' tips.

The results in Fig. 2 and 3 show that the nonlinear response is determined by the strength and distribution of the near-field caused by the excitation of a higher-order localized surface plasmon mode. The calculated profiles match the experimentally observed hot-spots and polarisation dependence.

In addition, Fig. 4 shows the 2PF and SHG intensity in function of the plane of polarisation of the incident light, for each triangle tip. Indeed, in all cases, the strongest 2PF and SHG response is found when the plane of polarisation is oriented perpendicularly to the tip direction.

For the SHG polar plots the signal-to-noise ratio is limited. In ESI† we added SHG-images and corresponding polar plots, that were taken with the SHG-microscope with a lower spatial resolution to gain a higher signal-to-noise ratio. In the ESI† figures the polar plots show more clearly that the SHG-intensity is strongest when the plane of polarisation of the incident light is oriented perpendicularly to the direction of the tip.

The 2PF and SHG intensity as a function of incident polarisation (Fig. 4) corresponds nicely with the calculated electric field profiles for different polarisations. The SHG and 2PF responses follow the spatial distribution of the optical near-fields, induced by the size, shape and orientation of the triangles within an array. For example, the horizontal polarisation (Fig. 3a and b) shows stronger localisation of the electric field on the tips of the triangle side perpendicular to the polarisation, similar to the SHG and 2PF responses (Fig. 4, data corresponding to tip 1). Similarly, for vertical polarisation (Fig. 3b) the field is stronger for the tip opposite the side parallel to the polarisation, similar to the SHG and 2PF responses (Fig. 4, data corresponding to tip 2 and 3). The differences in near-field distribution within triangles for different polarisations of the

incident light result in different intensity of SHG signal and 2PF as a function of polarisation. These results show that the near-field strength and profile of the higher order plasmon resonance fully determines the SHG and 2PF responses of the gold triangles. The presented results additionally confirm the previously published observation about the effect of the higher order mode on femtosecond patterning.^{22,24}

Furthermore, we investigate to which extent the generated SHG- and 2PF-light is polarised. In Fig. 5 we show 2PF-images (with lower spatial resolution as compared to Fig. 2 to obtain a higher signal-to-noise ratio) without analyzer (a–c), with an analyzer that transmits horizontally polarised light (d–f) or vertically polarised light (g–i), respectively. In Fig. 6 we show the corresponding SHG-images. During image capture, the camera recorded for each pixel the intensity on that pixel added with the intensity on the four neighbouring pixels. This leads to a lower spatial resolution, but a significantly higher signal-to-noise ratio.

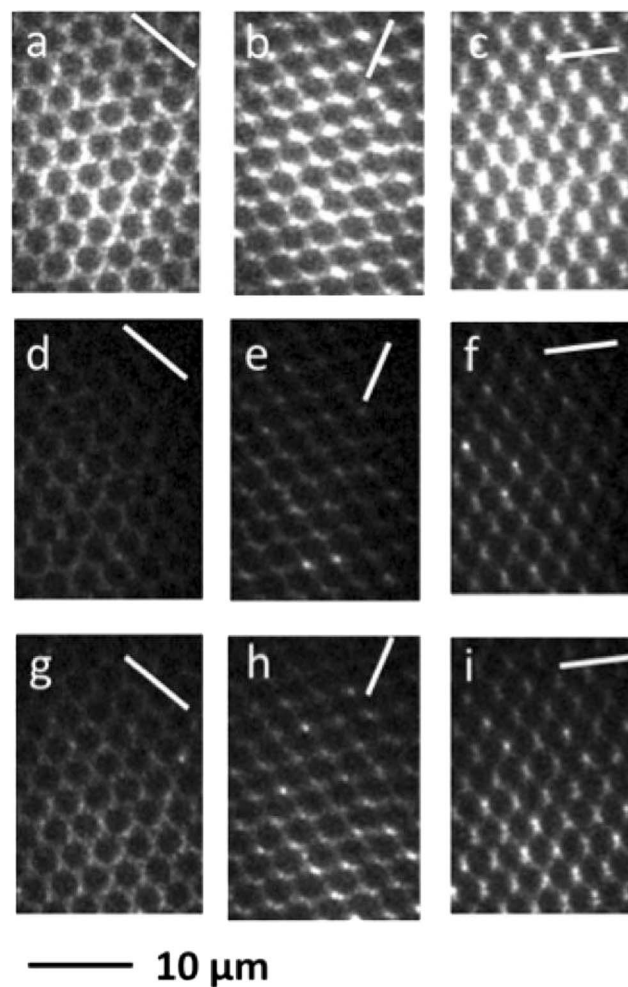


Fig. 5 Measured 2PF-images of the Au-triangles. The plane of polarisation of the incident light is depicted by the white bar on each image. Images (a–c) are taken without analyzer, while (d–f) and (g–i) are taken with an analyzer that transmits horizontally and vertically polarised light, respectively.

For SHG, when the plane of polarisation of the incident light is close to parallel with the plane of polarisation of the detected SHG-light (the case in Fig. 6f and h), a significant amount of SHG is detected. In contrast, when the plane of polarisation of the incident light is close to perpendicular to the plane of polarisation of the detected light (Fig. 6e and i), hardly any SHG-light is detected. This means that the generated SHG-light is strongly polarised, and the plane of polarisation of the generated light corresponds to the plane of polarisation that generates the SHG-light.

When we make the same comparison for the 2PF-images (comparing Fig. 5e with h, and Fig. 5f with i), the 2PF-intensity is hardly affected by the orientation of the analyzer. This shows that the generated 2PF is largely unpolarised. These results are understandable, as SHG is essentially a coherent process, leading typically to polarised SHG-light, while 2PF is a non-coherent process that commonly creates unpolarised light.

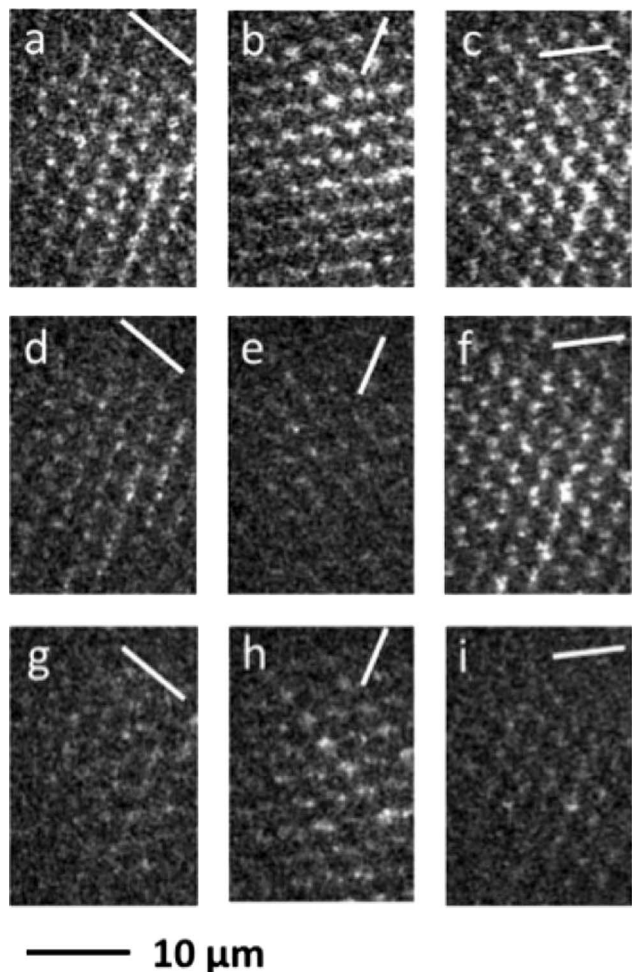


Fig. 6 Measured SHG-images of the Au-triangles. The plane of polarisation of the incident light is depicted by the white bar on each image. Images (a–c) are taken without analyzer, while (d–f) and (g–i) are taken with an analyzer that transmits horizontally and vertically polarised light, respectively.

III. Conclusion

In conclusion, we experimentally prove that the higher order mode of the plasmonic arrays can be used to enhance the nonlinear optical response. Additionally, we observe an atypical polarisation dependence of the SHG caused by a higher order plasmonic resonance that matches well with simulated near-field profiles. Furthermore, we confirm that the communication between the triangles is negligible due to the large distance between their tips, so that the recorded optical response is localised within hot-spots at triangle tips. In the end, this study shows that the simplicity of the nanosphere lithography technique and the strength of the higher order resonance could be used for many applications in which the enhancement of nonlinear optical processes as well as control of the polarisation direction is needed.

IV. Methods

Transmission spectroscopy

The transmission spectroscopy was measured using a Perkin-Elmer Lambda 900 UV-vis-NIR spectrophotometer.

Scanning electron microscope

Scanning electron microscope (SEM) images were recorded on a field-emission scanning electron microscope (FESEM, EOL JSM-6700F).

Nonlinear optical microscope

The light source is a Ti-sapphire laser (Spectra-Physics, Tsunami, 100 fs pulses with a repetition rate of 80 MHz). The wavelength of 800 nm is chosen. A Glan-Taylor polarizer is placed in the beam path, after which a zero-order half-wave plate for 800 nm (Thorlabs) is placed. By rotation of the half-wave plate, the plane of polarisation of the laser light incident on the sample can be changed. A longpass red filter (Schott, RG665, 1 mm) blocks transmittance of second-harmonic light generated by the optics earlier in the beam path and inside the laser. A lens ($f = 7.5$ cm) is positioned such that the spotsize plane has a diameter of 500 μm . The following parts are part of an inverted microscope (Olympus, IX71): the objective, a filter carousel and a tube to which the camera is connected. As objective a 100 \times oil-immersion objective was used. The filter set for the second-harmonic light consists of a bandpass filter (Schott, BG39, 2 mm) and an interference filter (Melles-Griot, F10-400, centre wavelength 400 nm, FWHM 10 nm). The filter set for the two-photon fluorescence transmits light from 420–650 nm. If applicable, a Glan-Taylor analyzer was placed in front of the filter set. The transmitted light is detected by an EM-CCD camera (Hamamatsu, C9100-13). Data were collected and analyzed with the HoKaWo software package provided with the camera.

Simulations

The simulations are performed with COMSOL Multiphysics 4.4, a commercial finite element based software package. The

1 symmetry of the lattice and the studied polarisation allow us to
2 reduce the computation on one cell using proper boundary
3 conditions as depicted in Fig. 3. The gold triangles are shaped
4 *via* a 3000 nm diameter sphere. The three sides of the basis
5 triangle are 900 nm long. The vertical 40 nm thickness is grown
6 along the sphere, this curvature leads to the top triangle being
7 slightly smaller than the basis triangle (see ESI† for a detailed
8 depiction). The mesh grid is maximum 10 nm wide in the gold,
9 130 nm in the air and 90 nm in the glass substrate. The latter is
10 optically described by a refractive index of 1.5 and gold
11 parameters are taken from Palik.²⁹

Acknowledgements

15 All authors warmly acknowledge R. Morarescu (UMONS, UGent)
16 for providing samples for preliminary investigations. B.K.
17 acknowledges financial support from SmartFilm Grant 830039
18 (ECV12020020892F) in the framework of the Convergence
19 Project and from FRS-FNRS. Furthermore, B.K. fully acknowl-
20 edges fruitful discussions with Prof. P. Damman (UMONS). G.R.
21 and B.M. acknowledge financial support from the Belgian
22 Science Policy Office under the project “Photonics@be” (P7-35)
23 in Belgium. T.V. and M.K.V. acknowledge the financial support
24 of the KU Leuven (GOA and PDM). BK, BM and TV acknowledge
25 support from the COST MP1403 project.

References

- 1 Z. Jacob, *MRS Bull.*, 2012, **37**, 76.
- 2 M. Kauranen and A. V. Zayats, *Nat. Photonics*, 2012, **6**, 737.
- 3 D. Lanterbecq, R. V. Deun, R. Morarescu, P. Damman and B. Kolaric, *Opt. Commun.*, 2013, **152**, 308.
- 4 P. Fauche, S. Ungureanu, B. Kolaric and R. A. L. Vallee, *J. Mater. Chem. C*, DOI: 10.1039/c4tc01787k, accepted.
- 5 A. Abass, S. R. K. Rodriguez, T. Ako, T. Aubert, M. Verschuuren, D. Van Th ourhout, J. Beeckman, Z. Hens, J. Gomez Rivas and B. Maes, *Nano Lett.*, 2014, **14**, 5555.
- 6 S. Ungureanu, B. Kolaric, J. Chen, R. Hillenbrand and R. A. L. Vallée, *Nanophotonics*, 2013, **2**(3), 173.
- 7 F. Tam, G. P. Goodrich, B. R. Johnson and N. J. Halas, *Nano Lett.*, 2007, **7**, 496.
- 8 N. Halas, *et al.*, *Chem. Rev.*, 2011, **111**, 3913.
- 9 S. Kim, J. Jin, Y.-J. Kim, I.-Y. Park, Y. Kim and S.-W. Kim, *Nature*, 2008, **453**, 757.
- 10 M. Agio and A. Alu, *Optical Antennas*, Cambridge University Press, 2013.
- 11 R. Micheletto, H. Fukuda and M. Ohtsu, *Langmuir*, 1995, **11**, 3333.
- 12 F. Burmeister, *et al.*, *Langmuir*, 1997, **13**, 2983.
- 13 R. Morarescu, H. Shen, R. A. L. Vallee, B. Maes, B. Kolaric and P. Damman, *J. Mater. Chem.*, 2012, **22**, 11537.
- 14 K. D. Ko, *et al.*, *Nano Lett.*, 2011, **11**, 61.
- 15 S. Viarbitskaya, *et al.*, *Nat. Mater.*, 2013, **12**, 426.
- 16 L. E. Hennemann, *et al.*, *Beilstein J. Nanotechnol.*, 2012, **3**, 674.
- 17 T. W. Ebbesen, *Nature*, 2006, **440**, 5.
- 18 J. Grandidier, *et al.*, *Nano Lett.*, 2009, **9**, 2935.
- 19 H. Husu, *et al.*, *Nano Lett.*, 2012, **12**, 673.
- 20 V. K. Valev, *et al.*, *Nano Lett.*, 2009, **9**, 3945.
- 21 V. K. Valev, *et al.*, *ACS Nano*, 2011, **5**, 91.
- 22 A. Kolloch, T. Geldhauser, K. Ueno, H. Misawa, J. Boneberg, A. Plech and P. Leiderer, *Appl. Phys. A*, 2011, **104**, 793.
- 23 R. Morarescu, L. Englert, B. Kolaric, P. Damman, R. A. L. Vallee, T. Baumert, F. Hubenthal and F. Trager, *J. Mater. Chem.*, 2011, **21**, 4076.
- 24 V. K. Valev, *et al.*, *Opt. Lett.*, 2013, **38**, 2256.
- 25 P. Yang, H. Portales and M. P. Pileni, *J. Phys. Chem. C*, 2009, **113**, 11597.
- 26 K. L. Shuford, M. A. Ratner and G. C. Schatz, *J. Chem. Phys.*, 2005, **123**, 114713.
- 27 S. Van Cleuvenbergen, G. Hennrich, P. Willot, G. Koeckelberghs, K. Clays, T. Verbiest and M. van der Veen, *J. Phys. Chem. C*, 2012, **116**, 12219.
- 28 M. van der Veen, B. Sels, D. De Vos and T. Verbiest, *J. Am. Chem. Soc.*, 2010, **132**, 6630.
- 29 E. D. Palik, *Handbook of Optical Constants of Solids*, Academic Press, New York, 1985.